Magnetic-Fluid Oscillator: Observation of Nonlinear Period Doubling

J.-C. Bacri, U. d'Ortona, and D. Salin
Laboratoire d'Acoustique et Optique de la Matière Condensée, Université Pierre et Marie Curie, Tour 13, 4 place Jussieu, 75252 Paris CEDEX 05, France
(Received 12 December 1990)

The peak pattern of a magnetic fluid, in both a vertical dc and an additional vertical ac magnetic field, behaves as an oscillator. Using the ac-dc field ratio as a control parameter, we study the dynamics of this oscillator. For low values, the peaks oscillate at the ac field frequency, whereas for a large enough value the oscillation is subharmonic (period doubling). The phase diagram is interpreted in terms of a bounded parametric resonance driven by the nonlinearity of the oscillator. In 2D this transition occurs with symmetry breaking from a triangular to a square pattern.

PACS numbers: 47.20.−k, 47.35.+i, 75.50.Mm

Understanding the routes to turbulence and chaos[1-3] requires well-defined experimental systems with convenient control parameters. The different classes of physical systems include Rayleigh-Bénard convection[4-6] or Taylor-Couette experiments,[7] Faraday's experiment[8-10] (parametric generation of surface waves on a horizontal layer of fluid vertically vibrated), sand pack vibrations,[8,11,12] and dielectric[13] or magnetic fluid[14,15] in an alternating electric or magnetic field. The subharmonic response of these systems allows observation of temporal and spatiotemporal chaos.[16,17] The subharmonic parametric excitation is driven by the harmonic time variation of one of the oscillator parameters: This excitation generally yields a first-order transition with threshold and hysteresis from a nonoscillating state to a subharmonic oscillation. As noticed a century ago,[9,18] subharmonic response can be also achieved through nonlinearities of the oscillator (the drive appears as an external force), in which case a second-order transition (Hopf bifurcation) occurs between a harmonic oscillation and a subharmonic one.

In this Letter, we report the first observation of the subharmonic response of a driven nonlinear magnetic-fluid oscillator. For a large enough applied vertical constant magnetic field, the free surface of a magnetic fluid becomes unstable, yielding a regular peak pattern.[19,20] This is our basic oscillator. We study the dynamic response of this peak pattern to an alternating vertical magnetic field added to the previous direct one; the ratio between the two fields is the control parameter of the experiment. The phase diagram is determined in a 1D geometry. Strikingly, the 2D version of the experiment shows a symmetry breaking, at the transition, from a triangular to a square pattern.

The magnetic fluid is a ferrofluid,[21,22] a colloidal suspension of magnetic grains stabilized by screened electrostatic repulsion.[23] Its magnetic behavior is paramagnetic with initial relative permeability $\mu_r=7$. The characteristics of the fluid are density $\rho=1.5\times10^3$ kg m^{-3}, viscosity $\eta=10^{-2}$ kg m^{-1} s^{-1}, and interfacial tension $\gamma=30$ mJ m^{-2} against air. In order to force a one-dimensional peak pattern, the fluid is contained in a thin (0.5 cm) and long (10 cm) groove of V cross section, made of Teflon nonwetted by the ferrofluid. The vessel is in between two coils in the Helmholtz position (field homogeneity better than 1% over the groove length). Increasing the vertical continuous magnetic field from zero, the magnetic-fluid interface remains flat until we reach a critical magnetization of the fluid, $M_c=5.5$ kA m^{-1}, at which point a line of equidistant peaks appear (Fig. 1). The height of the peaks is of the order of the critical wavelength $\lambda_c=0.9$ cm. We have already demonstrated[20] that this transition is first order. The measured values of M_c and λ_c are in reasonable agreement with the theoretical ones computed from the ρ, μ_r, and γ values.[19] We keep the static magnetic field constant at $M_0=8$ kA m^{-1}, well above M_c; the row of peaks is definitively set up: We will follow the time dependence of this regular peak pattern as forced by an additional small vertical alternating magnetic field of frequency Ω [corresponding magnetization $m_0\cos(\Omega t)$, total applied magnetization $M_0+m_0\cos(\Omega t)$]. For small values of the control parameter, $m=m_0/M_0$ ($m<0.1$), the row of peaks oscillates with the applied Ω frequency, all peaks vibrating in phase. The larger the value of m, the larger the amplitude a of vibration. These features have been observed over a wide range of frequency (Ω from 1 to 12 Hz). The peak pattern behaves as an oscillator, the characteristics of which can be estimated from the amplitude of oscillation versus frequency at a given m value ($m<0.1$). The resonance frequency in this linear regime coincides with the natural frequency obtained by shaking the vessel mechanically or with a field and letting it relax naturally at fixed M_0 and $m=0$. The level of superharmonic (2Ω) oscillation leads to the first anharmonicity.[24] For a given frequency of this wideband oscillator, as we increase the control parameter m, the oscillation of the peaks progressively loses its regularity; peaks neither vibrate in phase with each other nor with the Ω frequency. This dynamics is diffi-

 © 1991 The American Physical Society

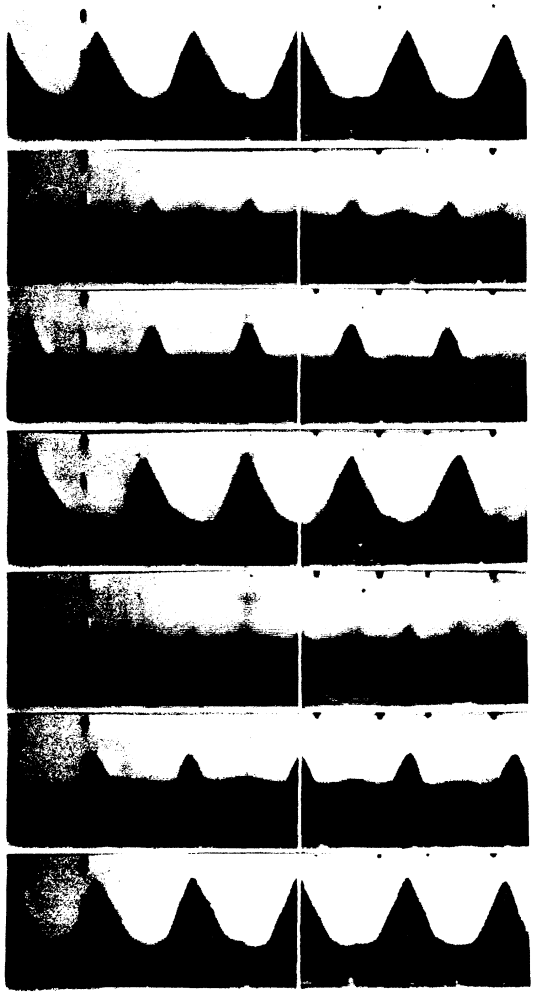

FIG. 1. Side views of peak rows in the period-doubling regime; $m=0.2$, $\Omega/2\pi=5$ Hz ($T=0.2$ s). From top to bottom, time $t=0$, 0.08, 0.12, 0.20, 0.28, 0.32, and 0.4 s ($=2T$). The white line is a video frame. The wavelength $\lambda=0.9$ cm.

cult to analyze. As we further increase m, we again get a regular pattern but at a period $2T$ (frequency $\Omega/2$). In Fig. 1, the excitation frequency is $\Omega=5$ Hz ($T=0.2$ s) and $m=0.2$. From top to bottom in the four first pictures, the initial peak row decreases, vanishes, and is replaced by a peak row for which peak positions are in previous valleys and vice versa. At time $T=0.2$ s (middle) the peak row is exactly out of phase with the top picture. As time increases further the system evolves to a pattern analogous to the top one; a complete cycle takes 0.4 s $=2T$ (frequency 2.5 Hz). We have definitively observed a subharmonic temporal oscillation. In Fig. 2, we plot the experimental phase diagram, control parameter m versus excitation frequency Ω. The circles (close to the line) are the upper limit of m of the harmonic oscillation (excitation T, oscillation T) whereas, the crosses are the lower bound of the subharmonic oscillation (excitation T, oscillation $2T$); in the region in between, the two modes compete leading to a kind of beating. The saliant features of our experiment, harmonic and subharmonic temporal oscillation with a soft transition between the two regimes, are reminiscent of a second-order subharmonic response through the nonlinearities of the oscillator.

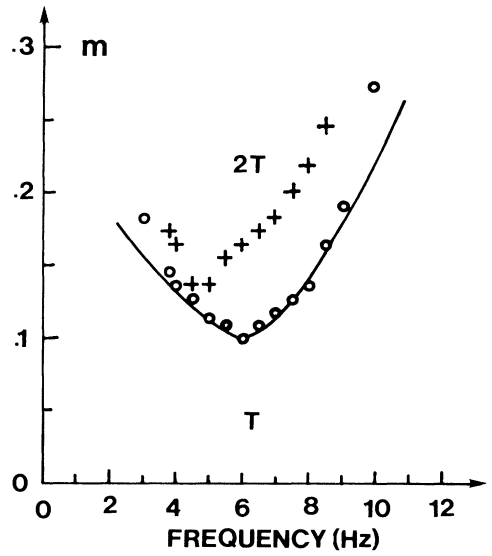

FIG. 2. Phase diagram of the peak dynamics. The control parameter m is the ratio of the amplitude of the alternating applied magnetic field to the dc field; $\Omega/2\pi$ is the frequency. Circles are the upper bound of harmonic oscillation, the line is the theoretical limit, and crosses denote the lower bound of the subharmonic regime (Fig. 1).

In order to try to account for the phase diagram, we derive the oscillator evolution equation from a very simple expression of the energy of the peak pattern. Let us focus on a basic spatial cell of the pattern consisting of the magnetic-fluid volume in between the white line and the nearest (left or right) valley in the top panel of Fig. 1 (half a spatial wavelength). For such an elementary volume, using simple dimensional arguments, we get[20] the variation of energy E from a flat interface to a peak of height p:

$$E=\Gamma p^2-H^2p^3+Gp^4, \tag{1}$$

where the three parameters $\Gamma\sim\gamma$, $G\sim\rho g$, and $H^2\sim\mu_0M^2$ include geometrical factors depending on the peak shape (close to a cone of 45° angle). Such a simple analysis was good enough to account for the hysteresis of the first-order static transition of the peak.[20] Minimization of (1) at a given applied magnetic field (corresponding to a magnetization M_0) gives the peak height p_0 ($2\Gamma-3H^2p_0+4Gp_0^2=0$). Considering a small magnetization, $m_0\cos(\Omega t)$, added to M_0, we can expand the energy (1) in the vicinity of (M_0,p_0); from Euler and Lagrange, we derive the time-dependent equation for

peak height variations $\delta p = p - p_0$:

$$\ddot{y} + 2\lambda\dot{y} + \omega_0^2 y = fm\cos(\Omega t) - \alpha y^2 - \beta y^3, \quad (2)$$

where $y = \delta p/p_0$ and the overdot denotes time derivative. The forcing f involves the derivative of E against M. The resonance frequency ω_0 and the two anharmonicities (α and β) involve respectively second, third, and fourth derivatives of E against p. All derivatives are taken at (M_0, p_0); λ is the viscous damping and $m = m_0/M_0$ the control parameter.

Equation (2) describes a nonlinear forced oscillator.[24] From the experiment, the harmonic and superharmonic responses yield the characteristics of our magnetic-field oscillator: $\omega_0/2\pi = 5.5 \pm 1$ Hz, $\lambda \simeq (0.3 \pm 0.1)\omega_0$, $f \simeq (0.5 \pm 0.1)\omega_0^2$, and $\alpha \simeq (15 \pm 5)\omega_0^2$; an estimate of β is $\beta \simeq (10 \pm 5)\omega_0^2$. With such an experimental determination of the parameters involved in Eq. (2), we get rid of questionable calculations carried out from Eq. (1). Equation (2) allows subharmonic oscillation, but, as opposed to classical parametric resonance excitation, governed by the nonlinearity (Duffin instead of Mathieu equation[9,18]). Following the discussion of (2) in the classical textbook,[24] but including the effect of large damping, the first-order ($y = y^{(1)} + y^{(2)} + \cdots$) solutions of (2) are harmonic oscillations, $y^{(1)} = a\cos(\Omega t)$ (an appropriate definition of t eliminates the phase factors in $y^{(1)}$ and $y^{(2)}$ in the regime where there are clean harmonic or subharmonic responses; the mixed regime is, of course, more complex), the amplitude of which is given through

$$a[(\omega_0^2 - \Omega^2)^2 + 4\lambda^2\Omega^2]^{1/2} = fm. \quad (3)$$

In the time-evolution equation of the second-order term $y^{(2)}$, the first anharmonicity contributes as $2\alpha y^{(2)} a\cos(\Omega t)$ which imitates classical parametric excitation with an intensity $h = 2\alpha a/\omega_0^2$: Above a threshold ($h > 4\lambda/\omega_0$), at which excitation overcomes viscous loss, a subharmonic oscillation, $y^{(2)} = b\cos(\Omega t/2)$, is allowed to develop with a well-defined amplitude b [because of nonlinearities, as b increases, the oscillator resonance frequency shifts from ω_0 to $\omega_0 + \chi b^2$, $\chi(\omega_0, \alpha, \beta)$,[24] leading to a saturation of b]. b is one of the roots of

$$[(\omega_0 + \chi b^2)^2 - \Omega^2/4]^2 + \lambda^2\Omega^2 = \alpha^2 a^2. \quad (4)$$

At a given frequency Ω, as m (and then a) is increased, b increases monotonously from zero at the threshold; subharmonic response results from bifurcation from the harmonic one: The T-$2T$ transition is a Hopf bifurcation. The marginal curve of the transition ($b = 0$) is computed from (3) and (4). We get the continuous line drawn in Fig. 2 close to the experimental data; this surprisingly good fit is obtained with the only adjustable parameter, on the vertical axis, $\alpha f = 5.0\omega_0^4$, to be compared to the value $\alpha f \sim 8\omega_0^4$ that we get from the measured characteristics of our magnetic-field oscillator. (We note that the error bars in the estimate of α and f are such that the two values are quite consistent with each other.) This is, indeed, a strong support to our theoretical interpretation. We have to notice that the large damping is responsible for the minimum of this curve being in the vicinity of ω_0. If our small-amplitude approach ($b \sim 0$) is well suited for determining the harmonic upper limit of the phase diagram, the lower bound of the subharmonic zone requires a much more complicated analysis which has not yet been achieved.

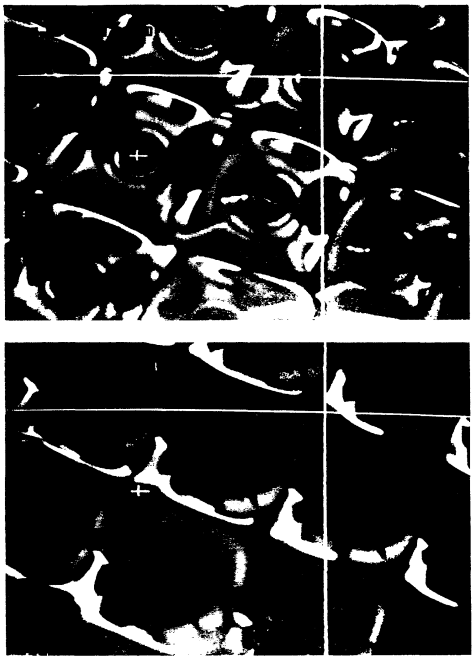

FIG. 3. Top view of the subharmonic 2D square peak pattern; $m = 0.2$, $\Omega = 5$ Hz. Top, $t = 0$ or $2T$; bottom, $t = T = 0.2$ s. White lines and crosses are video frames.

Even though it demonstrates the nature of the subharmonic transition, the one-dimensional geometry inhibits any kind of geometric effects. For that purpose we have also used a large rectangular vessel. Above a critical static magnetization, we do observe the classical triangular pattern of peaks.[19] This triangular geometry is chosen by the system for harmonic oscillation when an alternating magnetization is added to the constant one. For large enough m the spatial structure is no longer well defined, whereas increasing m further yields subharmonic (period $2T$) oscillation but with a square pattern (Fig. 3: top is $t = 0$ or $2T$, and bottom, $t = T$; the bottom pattern is in spatial phase opposition with the top picture). The spatial periodicity of nearest-neighbor peaks is 1.5 cm in both directions, leading to a wavelength $\lambda \sim 1.0$ cm analogous to the one of the 1D peak row. To account for the symmetry breaking from a T triangular pattern to a $2T$ square one, we first have to notice that the triangular lattice is the more stable at the static transition threshold, but could become metastable against the square one;[25] this transition has been observed under

unsteady conditions.[26] Moreover, a $2T$-oscillation regime requires the fluid to flow easily from a structure ($t=0$ or $t=2T$, top panels of Fig. 1 or 3) to one of opposite phase ($t=T$, Fig. 1 middle or Fig. 3 bottom). The simplest lattice with two sublattices (bipartite) is the square lattice. Extensions of this work to annular geometry (one-dimensional system with periodic boundary conditions) and 2D geometry are still in progress.

The peak pattern of a magnetic-fluid interface, under a constant vertical magnetic field, behaves as an oscillator when an additional vertical alternating field is applied. For low values of the control parameter, the peaks oscillate in phase at the excitation frequency. For large values the oscillation is subharmonic (period of twice the excitation period). In two dimensions the harmonic oscillation occurs in a triangular pattern whereas the subharmonic one occurs in a square lattice. The phase diagram and the main features of the experiment support the interpretation of a second-order transition from harmonic to subharmonic response achieved through the nonlinearities of the oscillator.

The authors benefited from stimulating discussions with Professor J. Banavar, Y. Couder, and M. Rabaud. Laboratoire d'Acoustique et Optique de la Matière Condensée is associated with the Centre National de la Recherche Scientifique.

[1]J. Ruelle and F. Takens, Commun. Math. Phys. **20**, 67 (1971).

[2]C. Tresser and P. Coullet, C. R. Acad. Sci. Paris **278A**, 577 (1978).

[3]M. Feigenbaum, J. Stat. Phys. **19**, 25 (1978); **21**, 669 (1979); Phys. Lett. **74A**, 375 (1979).

[4]J. P. Gollub and S. V. Benson, Phys. Rev. Lett. **41**, 625 (1978).

[5]J. Maurer and A. Libchaber, J. Phys. (Paris), Lett. **41**, L515 (1980).

[6]M. Dubois and P. Bergé, Phys. Ser. **33**, 159 (1986).

[7]M. Gorman and H. L. Swinney, Phys. Rev. Lett. **43**, 1871 (1979).

[8]M. Faraday, Philos. Trans. Roy. Soc. London **52**, 229 (1831); **52**, 319 (1831).

[9]Lord Rayleigh, Philos. Mag. **15**, 229 (1883); **16**, 50 (1883); **24**, 145 (1887).

[10]R. Keolian, L. A. Turkevich, S. J. Putterman, I. Rudnick, and J. A. Rudnick, Phys. Rev. Lett. **47**, 1133 (1981).

[11]S. Douady, S. Fauve, and C. Laroche, Europhys. Lett. **8**, 621 (1989).

[12]P. Evesque and J. Rajchenbach, Phys. Rev. Lett. **62**, 44 (1989).

[13]V. A. Briskman and G. F. Shaidurov, Dokl. Akad. Nauk SSSR **180**, 1315 (1968) [Sov. Phys. Dokl. **13**, 540 (1968)].

[14]M. P. Perry and T. B. Jones, J. Appl. Phys. **46**, 756 (1974).

[15]A. O. Cebers and M. M. Maiorov, Magn. Gidrodin. **4**, 38 (1989).

[16]S. Ciliberto and J. P. Gollub, Phys. Rev. Lett. **52**, 922 (1984); J. Fluid Mech. **158**, 382 (1985).

[17]A. B. Ezerskii, M. I. Rabinovich, V. P. Reutov, and I. M. Starobinets, Zh. Eksp. Teor. Fiz. **91**, 2070 (1986) [Sov. Phys. JETP **64**, 1228 (1986)].

[18]K. O. Friedrichs and J. J. Stoker, Q. Appl. Math. **1**, 97 (1943).

[19]M. D. Cowley and R. E. Rosensweig, J. Fluid Mech. **30**, 671 (1967).

[20]J.-C. Bacri and D. Salin, J. Phys. (Paris), Lett. **45**, L767 (1984).

[21]R. Rosensweig, *Ferrohydrodynamics* (Cambridge Univ. Press, London, 1985).

[22]J.-C. Bacri, R. Perzynski, and D. Salin, Endeav. New Ser. **12**, 76 (1988).

[23]R. Massart, IEEE Trans. Magn. **17**, 1247 (1981).

[24]L. D. Landau and E. R. Lifshitz, *Mechanics* (Pergamon, New York, 1958).

[25]A. Gailitis, J. Fluid Mech. **82**, 401 (1977).

[26]J. Weisfreid and D. Allais, in "New Trends in Nonlinear Dynamics and Pattern Forming Phenomena: The Geometry of Nonequilibrium," edited by B. Coullet and P. Huerre (Plenum, New York, to be published).